Brain (1998), **121,** 2189–2200

Parieto-occipital cortex activation during self-generated eye movements in the dark

Ian Law,[1] Claus Svarer,[1] Egill Rostrup[2] and Olaf B. Paulson[1]

[1]*The Neurobiology Research Unit, Copenhagen University Hospital, Rigshospitalet and* [2]*The Danish Research Centre for Magnetic Resonance, Hvidovre Hospital, Denmark*

Correspondence to: Ian Law, MD, The Neurobiology Research Unit, N 9201, Copenhagen University Hospital, Rigshospitalet, 9 Blegdamsvej, 2100 Copenhagen, Denmark. E-mail: ilaw@pet.rh.dk

Summary

A number of extrastriate visual areas in the parieto-occipital cortex are known from single-cell recordings of the macaque monkey to be involved in the coding of eye-position signals in the brain. These are important for the accurate location of visual objects in extrapersonal space. It can be predicted that these areas will show increased activation during the performance of eye movements at high frequency. In the present study PET and measurements of the regional distribution of cerebral blood flow (rCBF) were used as indirect measures of neural activity. Two independent groups of normal volunteers performed large-amplitude self-generated eye movements in complete darkness, thus removing the confounding effects of visual stimulation on parieto-occipital activation. The first group (group A; $n = 5$) served as a hypothesis-generating group and the second group (group B; $n = 4$) served as a hypothesis-testing group. The data were analysed using statistical parametric mapping at a significance level corrected for multiple comparisons (group A, $Z > 4.08$; group B, $Z > 4.04$). Significant rCBF increases were found for both groups in the frontal eye fields, supplementary eye fields, cerebellar vermis and putamina/thalami. Additionally, activation was found in the cunei in the posterior bank of the parieto-occipital sulcus. Also, the extraocular muscles were activated and, as a consequence of the partial volume effect, projected to the orbitofrontal cortices. At a less conservative threshold, activation was found close to the intraparietal sulci on the left side ($Z = 3.91$, $P = 0.09$) and right side ($Z = 3.33$, $P = 0.42$). The locations of these areas were confirmed in group B with reference to high-resolution structural MRI scans. The activation of the parieto-occipital cortex without overt visual stimuli is interpreted as the result of neural activity related to the reception of efferent copies of motor commands and/or the activation of neurons coding for eye position relative to the orbits. These are important constituents for the location and remapping of visual stimuli in space.

Keywords: saccade; frontal eye field; supplementary eye fields; cuneus; vermis

Abbreviations: AC = anterior commissure; EOG = electro-oculography; PC = posterior commissure; rCBF = regional cerebral blood flow; SPM = statistical parametric mapping

Introduction

Several mapping studies of the cerebral organization of areas involved in saccadic eye movements in the human have been performed using regional cerebral blood flow (rCBF)-based techniques (Melamed and Larsen, 1979; Fox *et al*., 1985; Paus *et al*., 1993, 1995; Anderson *et al*., 1994; Nakashima *et al*., 1994; O'Driscoll *et al*., 1995; O'Sullivan *et al*., 1995; Darby *et al*., 1996; Petit *et al*., 1996; Sweeney *et al*., 1996; Law *et al*., 1997). These have demonstrated the involvement of a widely distributed network including cortical and subcortical areas known through electrical stimulation, single-cell recordings and ablation studies in, for example, the cat and the monkey (Schall, 1991*a*).

The neurophysiological evidence suggests that large sections of the saccade-generating system have visual properties. These include some predominantly motor regions, such as the frontal eye fields (Schall, 1991*b*) and the supplementary eye field (Schall, 1991*c*). These areas are possibly involved in the target selection of a visually guided saccade. Conversely, some predominately visual areas in the parieto-occipital lobe [e.g. inferior parietal lobe, area V3A and area PO (V6)] are actively modulated by non-visual information, e.g. the angle of gaze (Andersen and Mountcastle, 1983; Galletti and Battaglini, 1989; Galletti *et al*., 1995). The gaze-dependent neurons in the parieto-occipital region might be involved in the construction of an internal map of the visual environment in which the

topographical position of the objects reflects their objective position in space instead of reflecting the retinotopic position of their images, thus functioning in encoding spatial locations of the field of view in a head frame of reference. Such an objective map of the visual world might allow the stability of visual perception despite eye movements (Galletti and Battaglini, 1989).

One obvious strategy to locate the non-visual activation components of these areas located in the dorsal visual stream during eye movements would be to perform self-generated eye movements in the dark. This has previously been performed using PET by Petit *et al*. (1993, 1996). However, in both of these studies no activation of visual areas in the dorsal visual stream was found when the task required the simple, on-line programming and execution of self-generated saccades in the dark. As the neurophysiological evidence suggests that the occipitoparietal cortex is involved, it seemed justified to challenge these negative findings.

In the present study we have repeated the paradigm using PET in two separate groups of normal subjects serving as hypothesis-generating and as hypothesis-testing data sets, respectively. Furthermore, in the hypothesis-testing group structural MRI scans were acquired to confirm the anatomical locations of activated areas in the individual subjects.

Materials and methods

The subjects consisted of strongly right-handed (Oldfield, 1971) normal volunteers and were divided into two groups. The first group (A) was the hypothesis-generating group and consisted of five subjects (median age, 24 years; range, 23–24 years; three females, two males). The second group (B) was the hypothesis-testing group and consisted of four subjects (median age, 21 years; range, 21–34 years; one female, three males). None of the subjects had past or present neurological or psychiatric disorders or actively used medication or recreational drugs. All had normal clinical examinations of visual acuity without correction and no ophthalmological disorders, such as strabismus, were present.

Informed consent was obtained according to the Declaration of Helsinki II and the study was approved by the local ethics committee of Copenhagen [J. Nr. (KF) 01–339/94].

Activation paradigm and behavioural control

The two conditions were the resting state with eyes closed and the performance of voluntary self-generated large-amplitude horizontal saccadic eye movements with the eyes open. Each scan was carried out in complete darkness for both conditions. This was achieved by fitting over the eyes a pair of black goggles that permitted the eyes to move around freely. Additionally the goggles were covered with dense black cloth and the scanner gantry was draped with a black curtain. A total of 12 scans were performed per subject, and each condition was presented in randomized order. However, for group A data from only six of the scans were used as the other six scans were reserved for unrelated paradigms. Thus, each condition was repeated three times in group A and six times in group B. Each subject was trained in the eye movement task for a few minutes prior to scanning.

Eye movement performance was recorded after 20 min of dark adaptation using direct current electro-oculography (EOG) at a sampling frequency of 1 kHz. The EOG signal was calibrated before and after the scan session to 13 LEDs (light-emitting diodes) at horizontal visual angles ranging from –60° to 60°. The interdiode visual angle was 10°. The resulting calibration curves were sigmoidal in shape, which allowed conversion of the EOG signal to visual angle by fitting a fifth-order polynomial to the curves.

PET scanning

PET scans were obtained with an 18-ring GE-Advance scanner (General Electric Medical Systems, Milwaukee, Wis., USA) operating in 3D acquisition mode, producing 35 image slices with an interslice distance of 4.25 mm. The total axial field of view was 15.2 cm with an approximate in-plane resolution of 5 mm. The technical specifications have been described elsewhere (DeGrado *et al*., 1994).

Every subject in the two groups received 12 intravenous bolus injections of 200 MBq (5.7 mCi) of $H_2{}^{15}O$ with an interscan interval of 10–12 min. The isotope was administered in an antecubital intravenous catheter over 3–5 s followed immediately by 10 ml of physiological saline for flushing. Head movements were limited by head-holders constructed from thermally moulded foam.

Before the activation session a 10 min transmission scan was performed for attenuation correction. Subjects were asked to initiate eye movements ~15 s before the isotope arrived at the brain, and they continued throughout the acquisition period of 90 s (Kanno *et al*., 1991). Images were reconstructed with a 4.0 mm Hanning filter transaxially and an 8.5 mm Ramp filter axially. The resulting distribution images of time-integrated counts was used as an indirect measure of regional neural activity (Fox and Mintun, 1989).

MRI scanning

Structural MRI scanning was performed with a 1.5 T Vision scanner (Siemens, Erlangen, Germany) using a 3D MPRAGE (magnetization prepared rapid acquisition gradient echo) sequence (TR/TE/TI = 11/4/300 ms, flip angle = 12°). The images were acquired in the sagittal plane with an in-plane resolution of 0.92 mm and a slice thickness 1.0 mm. The number of planes was 170 and the in-plane matrix dimensions were 256 × 256. MRI scans were obtained only for the subjects in group B.

Image analysis

For all subjects the complete brain volume was sampled. Image analysis was performed using statistical parametric

mapping software (SPM95, Wellcome Department of Cognitive Neurology, London, UK) (Frackowiak and Friston, 1994). All intra-subject images were aligned on a voxel-by-voxel basis using 3D automated six-parameter rigid-body transformation (AIR software) (Woods *et al*., 1992). In group B, PET-MRI coregistration was performed using AMIR (automatic multimodality image registration) (Ardekani *et al*., 1995). In both groups, transformation into the standard stereotaxic atlas of Talairach and Tournoux was performed based on the intra-individual average PET images (Friston *et al*., 1995*a*; Talairach and Tournoux, 1988). The stereotaxically normalized images consisted of 31 planes of $2 \times 2 \times 4$ mm voxels. Before statistical analysis, images were filtered with a 16 mm isotropic Gaussian filter to increase the signal-to-noise ratio and accommodate the residual variation in morphological and topographical anatomy that was not accounted for by the stereotaxic normalization process (Friston, 1994). Differences in global activity were removed by proportional normalization of global brain counts to a value of 50.

In the hypothesis-generating data set (group A), testing the null hypothesis rejecting regionally specific condition activation effects was performed by comparing the average of all saccade scans with all resting scans on a voxel-by-voxel basis. The resulting set of voxel values constituted a statistical parametric map of the t statistic, SPM{t}. By transforming values from the SPM{t} into the unit Gaussian distribution using a probability integral transform, changes could be reported in Z scores (SPM{Z}). Voxels were considered significant if their Z score exceeded a threshold of $P < 0.05$ after correction for multiple non-independent comparisons ($Z > 4.08$). This threshold was estimated according to Friston *et al*. (1991, 1995*b*) using the theory of Gaussian fields. The resulting foci were then characterized in terms of the number of voxels and peak Z score above this level. The threshold was subsequently dropped to $Z = 1.64$ (or $P < 0.05$ uncorrected) in order to observe activation tendencies and in particular to define activated areas in the parieto-occipital cortex.

Data for the independent hypothesis-testing group (group B) were analysed both for the group and individually. The single-subject analysis was performed to assess individual variability and increase precision of the anatomical location of cerebral activation. The replication values from the analysis for group B were acquired by sampling the Z scores on the peak coordinates of foci defined in the group A analysis, both as a group and individually, at a threshold value of $P < 0.05$ uncorrected. Furthermore, group B was analysed independently of group A at a threshold value of $P < 0.05$ ($Z > 4.04$) corrected for multiple non-independent comparisons, and the locations of these activated areas were subsequently located in the individual subjects at a threshold of $P < 0.05$ uncorrected.

Changes in rCBF measurements are confounded by global changes. This source of variance was accounted for in the present study by proportional normalization of global brain counts to a value of 50. By default the SPM software obtains the global values from the grey matter voxels by averaging only count values greater than 80% of the maximum. Furthermore, this threshold value also acts as a data reduction device, limiting the effective space where significant changes can be found. Using this standard setting, subsequent analysis revealed significant activations in regions close to the orbitofrontal cortices (see Results), which we suspected had an extracerebral origin (Drevets *et al*., 1992), e.g. increases in blood flow in the eye muscles. To investigate this further we performed single-subject analysis on the subjects in group B at the maximum resolution possible and projected the results onto the corresponding structural MRI scans for anatomical localization. These analyses were thus performed without the application of a Gaussian filter kernel, without reducing the volume by thresholding, and at a threshold of $P < 0.05$ uncorrected.

Results

Eye movements

In the resting state low-amplitude deflections of the eyes were observed. During the self-generated eye movement task the average number of movements per second for group A was 2.04 ± 0.22 (SD) and the amplitudes were 46.7 ± 6.9° (SD) for the right and 47.7 ± 3.3° (SD) for the left hemifield, respectively. For group B the corresponding values were 1.87 ± 0.33, and 48.4 ± 4.9° and 48.2 ± 4.2°. There was no significant difference between the number of eye movements performed for the two groups in a two-tailed unpaired t test [$P > 0.05$; $t(37) = 1.9$]. An example of the sampled EOG recordings from a single subject (subject 3, group B) in the time period immediately after the arrival of the $H_2{}^{15}O$ bolus at the brain can be seen in Fig. 1.

Activation patterns

Group A

The areas that were significantly activated during the performance of self-generated eye movements in group A are shown in Table 1 and Figs 2 and 3. The lower-case letters in square brackets in Table 1 refer to various cerebral structures defined in the legend of Table 1 and illustrated in Fig. 3.

In the frontal lobes the middle frontal gyri areas were activated, probably corresponding to the supplementary eye fields ([b] in Table 1) (Fox *et al*., 1985). Bilaterally, close to the precentral gyri, activated areas were seen extending from the frontal operculum to the middle frontal gyrus, fusing with the supplementary eye field activation on the right, probably corresponding to the frontal eye fields ([a]).

In terms of the number of activated voxels and the Z score, the activation of the cerebellum ([d]) was the greatest. The activation was centred on the medial structures without extension to the lateral cerebellar hemisphere and involved

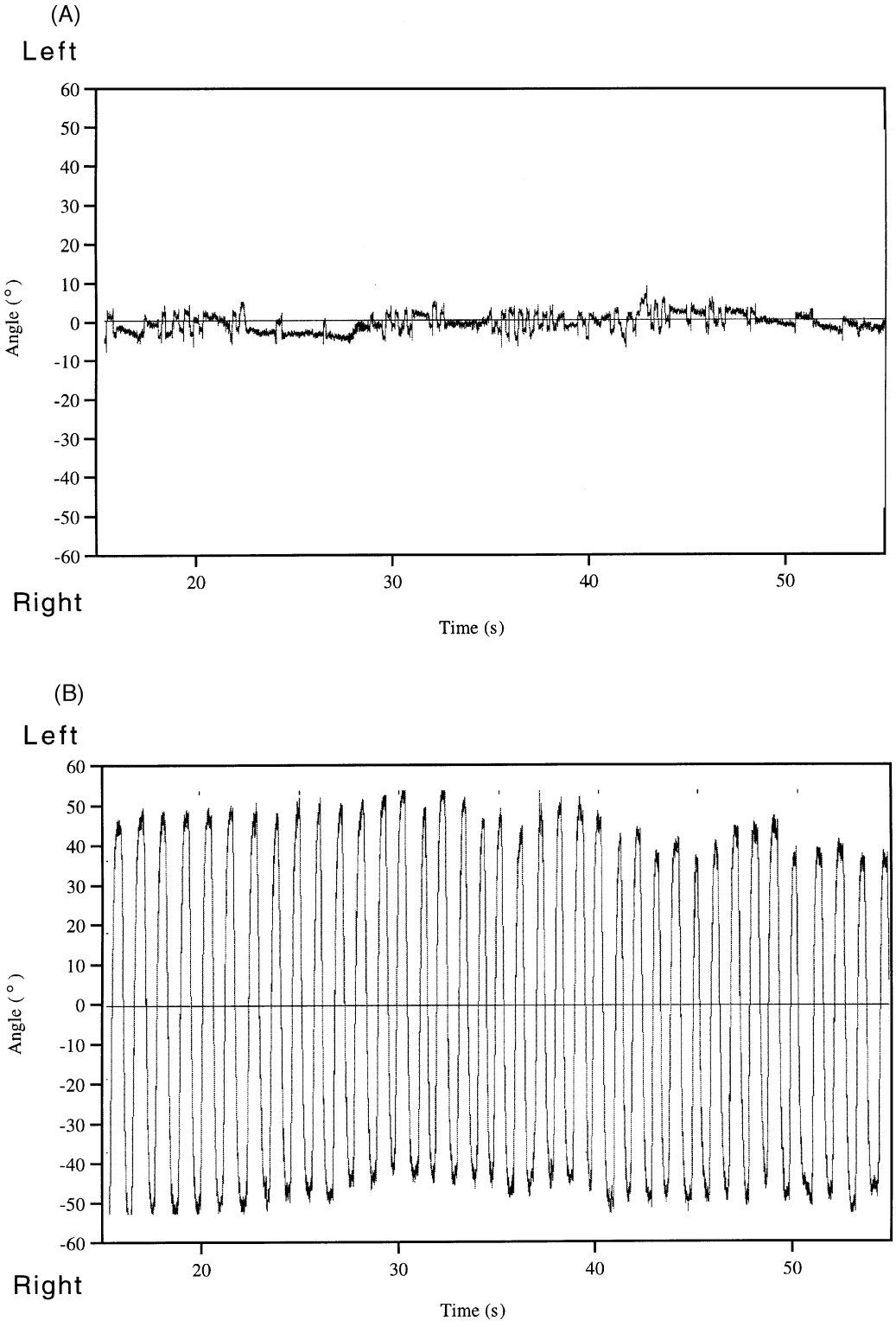

Fig. 1 A sample of horizontal EOG recordings in a single subject calibrated in degrees. In both rest (**A**) and self-generated eye movement (**B**) conditions, the $H_2{}^{15}O$ bolus reached the brain ~20 s after the initiation of the eye movements. It is behaviourally related rCBF events within the following 30 s that are mainly responsible for the activation pattern in that particular condition (Iida *et al*., 1991; Silbersweig *et al*., 1993).

Table 1 *Results from the hypothesis-testing group (B) showing group activations and the average of individual subject activations derived from the coordinates of activated areas from the hypothesis-generating group (A)*

	Region	Group A						Group B		
		Talairach coordinates			Size (voxels)	Extent of focus in *z* direction (mm)	*Z* score at peak activation	*Z* score at peak activation of Group A		No. of subjects
		x	*y*	*z*				Group	Individual $\bar{Z} \pm$ SD	
[a]	L FEF	–50	–2	36	795	12 → 56	4.82	2.88	2.6 ± 0.4	4
[a]	R FEF &	42	–8	48		12 → 60	5.33	4.30	2.3 ± 0.2	4
[b]	L & R SEF	4	–10	60	1637	48 → 68	5.73	4.04	3.5 ± 0.7	2
[c]	L putamen & thalamus	–20	–14	4	252	–4 → 16	4.75	3.30	2.2 ± 0.2	2
[c]	R putamen	22	–8	8			4.27	3.01	2.6 ± 0.3	2
[c]	R thalamus	20	–20	16	344	–4 → 20	3.19	4.11	2.1 ± 0.2	2
[d]	Vermis &	16	–64	–20			6.91	5.08	2.9 ± 0.8	4
[d]	Flocculus region &	–20	–54	–32			4.50	2.22	2.1 ± 0.0	3
[d]	Mesencephalon	–6	–38	–4	3639	–48 → 0	4.48	NS	NS	0
[e]	L orbit (eye muscles)	–18	28	–20	233	–24 → –12	6.32	6.54	3.3 ± 0.6	4
[e]	R orbit (eye muscles)	20	28	–20	398	–24 → –8	5.95	7.39	4.0 ± 1.0	4
[f]	L cuneus &	–12	–86	32			4.04	4.07	2.7 ± 0.9	3
[f]	R cuneus	8	–86	32	382	24 → 40	4.54	3.11	2.8 ± 0.6	3

Comparison of the self-generated eye movement scans with rest for groups A and B showing the anatomical regions of foci of significant change in normalized regional counts at a significance threshold of $P < 0.05$, corrected for multiple non-independent comparisons. The coordinates are given in the standard stereotaxic space (Talairach and Tournoux, 1988) in mm for the maximally significant pixel in each area in the order *x, y, z*; *x* is the lateral displacement from the midline (– for the left hemisphere and + for the right hemisphere); *y* is the anterior–posterior displacement relative to the anterior commissure (– for positions posterior to this); *z* is the vertical displacement relative to the AC–PC line (– below this line). The lower case letters in square brackets in this table and Fig. 3 refer to the following structures: a, FEF (front eye field); b, SEF (supplementary eye field); c, putamen/thalamus; d, cerebellum; e, eye muscles (artefact); f, cuneus. Interconnected foci are indicated by '&' and the total voxel counts above the threshold are given. The vertical (*z*) extension of the foci gives the number of continuous slices covered by the activated area. The values from group B are sampled from the analysis of the whole group and from the single subject analysis at the coordinates derived from the group A analysis. The number of subjects contributing with a *Z* value >1.64 ($P < 0.05$, uncorrected) to the calculated mean and standard deviation of the *Z* scores are given. L = left; R = right; NS = not significant; $\bar{Z}$ = mean of individual *Z* scores

the vermis, the dentate nuclei, the tonsillae cerebelli, the flocculi and the noduli vermis. At –12 to –4 mm below the anterior commissure–posterior commissure (AC–PC) line (Fig. 2) the left mesencephalon was activated close to the superior colliculus. The cerebellar activation kept within the boundaries of the cerebellum as defined by the atlas of Talairach and Tournoux (1988). Of other subcortical structures, the putamina and thalami ([c]) were activated bilaterally, merging into single foci, on the right in two separate peaks and on the left in a single peak.

In the posterior parieto-occipital cortices, bilateral symmetrical activation foci were seen immediately posterior to the parieto-occipital sulcus in the cuneus ([f]). Additionally, bilaterally in the cortex, close to the intraparietal sulci in the precunei, two foci above the threshold of $P < 0.05$, corrected, were found at (x, y, z) = (–20, –66, 52); $Z = 3.91$; $P = 0.09$, corrected, and (x, y, z) = (32, –58, 48); $Z = 3.33$; $P = 0.42$, corrected.

Two crescent-shaped increases ([e]) were seen bilaterally in the region of the orbitofrontal cortices. These represent blood flow increases in the eye muscles (see below).

Lowering the threshold for significant changes to $P < 0.05$ uncorrected did not reveal new activation foci in cerebral regions other than those already described. In particular there was no activation in the primary visual cortices.

Group B

With the exception of the mesencephalon, all activated areas defined at the peak *Z* score in group A were replicated in the analysis of group B. However, only the larger activated areas (frontal eye fields, vermis) were replicated in all of the individual subjects at this location (Table 1). When the peak coordinates were defined in group B independently of group A the same modules could be identified, but with the peak coordinate located at a vector distance ranging from 0 to 22 mm (Table 2). Although the coordinates of the putative frontal eye fields were located close to the cortex of the central sulcus according to the Talairach and Tournoux atlas (1988), the projections on the structural MRI scans showed that they were actually in the precentral gyrus region in all four subjects. It was further confirmed that the cunei were activated on the occipital banks of the parieto-occipital sulci (Fig. 4). Additionally, activation was found close to the right intraparietal sulcus (x, y, z) = (20, –76, 48); $Z = 5.54$; $P < 0.05$, corrected. Activation of the supplementary eye fields

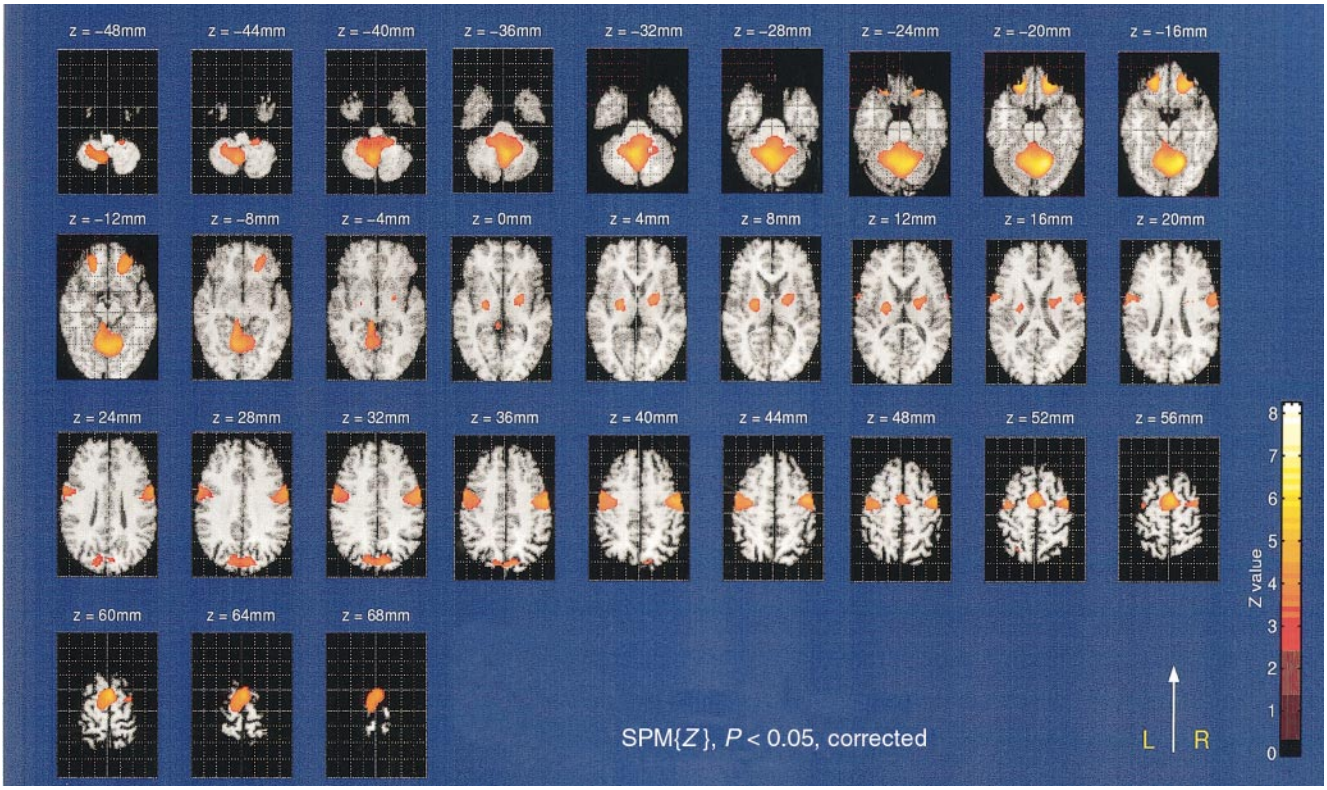

Fig. 2 Group analysis (SPM{*Z*}) of all saccade scans compared with rest in the hypothesis-generating group (group A). The spatial extent of significantly activated areas is for anatomical reference superimposed on a single MRI template in coregistration with the stereotaxic atlas of Talairach and Tournoux (1988). All images are displayed at a significance threshold of $P < 0$ 05, corrected. Group A: $n = 5$; 3 rest, 3 eye movement scans.

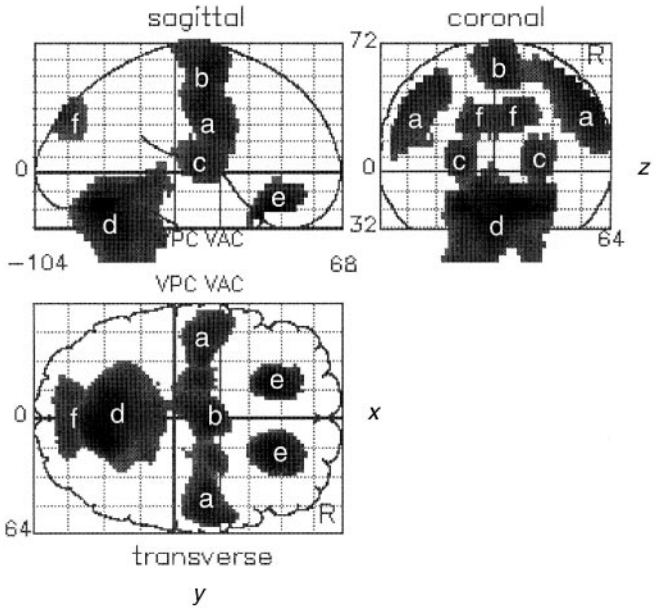

Fig. 3 Statistical parametric map (SPM{*Z*}) of the orthogonal projections for group A of the performance of eye movements versus rest ($P < 0.05$, corrected). The SPM projections correspond to the stereotaxic grid of Talairach and Tournoux (1988). VPC and VAC denote the vertical projections of the anterior and the posterior commissure, respectively. The lower-case characters refer to regions of activation given in the legend of Table 1.

and the subcortical structures could not be found in all subjects (Table 2).

The results from the single-subject analysis without the inclusion of additional filtering projected on to the structural MRI scans confirmed the suspicion that the orbitofrontal cortex activations arose from extracerebral structures, namely the eye muscles of the orbital cavities (Fig. 5). These had the largest *Z* scores when performing the analysis in this fashion. The activated areas were concentrated at the apex of the pyramidal shapes of the orbits and were located over the six external ocular muscles situated in the orbital fat.

Discussion

The results of this study confirm data from animal experiments regarding the involvement of parieto-occipital areas during the performance of saccades in the dark. In two independent groups, significant activation was found just posterior to the parieto-occipital sulcus in the cuneus. Although significant activation close to the right intraparietal sulcus was found in the hypothesis-testing group (B) independently, the intraparietal sulcus activations in the hypothesis-generating group (A) were not significant (Fig. 4). However, previous PET activations in this area during eye movements could endorse a less conservative approach (Petit *et al*., 1996). Besides these extrastriate visual areas, the other activated

Table 2 *Results from the hypothesis-testing group (B) showing group activations and the average of individual subject activations*

Region	Talairach coordinates at peak activation							*Z* score at peak activation		No. of subjects
	Group				Individual			Group	Individual $\overline{Z} \pm$ SD	
	x	*y*	*z*	***v***	*x*	*y*	*z*			
L FEF	–38	–16	48	22.0	–38 ± 3	–18 ± 3	47 ± 6	7.04	4.6 ± 0.8	4
R FEF &	42	–14	44	7.2	42 ± 10	–15 ± 7	37 ± 3	5.75	4.5 ± 0.4	4
L & R SEF &	–8	–12	60	12.2	–2 ± 5	–8 ± 4	56 ± 6	4.67	3.4 ± 0.9	3
L putamen &					–13 ± 4	–23 ± 7	11 ± 3		3.0 ± 1.1	4
L thalamus	–12	–26	12	16.5	–28	2	12	4.58	3.3	1
R putamen &					21 ± 1	–25 ± 3	8 ± 4		3.6 ± 0.1	2
R thalamus	20	–20	12	12.8	24 ± 2	–11 ± 3	11 ± 4	4.4	2.5 ± 0.7	3
Vermis &	6	–72	–20	12.8	–1 ± 4	–70 ± 2	–21 ± 7	7.39	4.3 ± 1.0	4
L flocculus region &	–16	–46	–48	18.3	–19 ± 4	–52 ± 3	–41 ± 7	5.05	2.6 ± 0.7	3
R flocculus region &	22	–42	–44		22 ± 2	–42 ± 4	–42 ± 6	5.12	3.8 ± 0.4	2
Mesencephalon								NS		0
L orbit (eye muscles)	–22	28	–20	4.0	–25 ± 4	24 ± 3	–23 ± 2	6.69	3.8 ± 1.0	4
R orbit (eye muscles)	30	22	–24	12.3	26 ± 4	25 ± 4	–22 ± 2	7.92	4.8 ± 0.7	4
L cuneus &	–12	–86	32	0.0	–15 ± 3	–86 ± 4	29 ± 2	4.42	3.1 ± 0.7	3
R cuneus	22	–86	32	14.0	21 ± 3	–88 ± 3	32 ± 5	5.56	3.4 ± 0.8	4

Results from an independent analysis of the subjects in group B, both as a group and as mean values of the single subject analysis. The nomenclature follows Table 1; ***v*** is the vector distance in mm between the coordinates of corresponding regions in groups A and B. FEF = frontal eye field; L = left; R = right; NS = not significant; SEF = supplementary eye field; $\overline{Z}$ = mean of individual Z scores.

areas are replications of and in concordance with the localization of the larger functional modules of the saccade generation system previously found during self-generated eye movements (Petit *et al*., 1993, 1996). These include the involvement and the location of the frontal eye fields in the cortex of the precentral gyri ([a]), the supplementary eye fields ([b]), the putamina and the thalami ([c]), and the cerebellar vermis in its entire vertical length ([d]). Not previously described was the possibility of confusing changes in eye-muscle blood flow with activation of the orbitofrontal cortices ([e]). The activation of the left mesencephalon was not present in both our groups.

There is ample evidence connecting the parietal lobe with visually guided saccadic eye movements in both the monkey and man (Andersen, 1987; Anderson *et al*., 1994). Previously activation of the inferior and posterior parietal lobes during eye movement-related paradigms has been found during the performance of visually guided saccades (Anderson *et al*., 1994; Law *et al*., 1997), during saccades to a remembered position (Anderson *et al*., 1994; O'Sullivan *et al*., 1995; Sweeney *et al*., 1996), during anti-saccades and conditional anti-saccades (O'Driscoll *et al*., 1995; Sweeney *et al*., 1996) and during imagined saccades to visual targets (Law *et al*., 1997). These areas are located along the dorsal visual stream, the 'where' pathway, and have, through behavioural and clinical studies, long been implicated in the internal mapping of spatial representations (Mishkin *et al*., 1983; Haxby *et al*., 1991). Furthermore, the posterior superior parietal lobes close to the cunei have been found to be activated during the performance of prelearned sequences of saccades from memory in the dark (Petit *et al*., 1996), possibly related to saccade planning or the intention of saccade performance (Gnadt and Andersen, 1988; Barash, 1997).

Activations in the cunei as individual local maxima have not been described in PET studies of visually guided saccades (Anderson *et al*., 1994; Law *et al*., 1997). This is presumably due to the partial volume effect promoted by the image smoothing with broad filter kernels (10–20 mm) involved in the statistical analysis. The cunei are present, but will appear in the dorsal tail of a large occipital activation including neighbouring striate and extrastriate cortices.

The above-mentioned PET studies have found activation in the posterior parietal lobes both bordering and including the cunei. These activations can be attributed to either visuospatial or memory components, which were not present in our experiment. Interpretations of the extrastriate visual cortical activations found in our non-visual motor task could include several possibilities. These areas could themselves send motor command signals (Mountcastle *et al*., 1975) or represent motor intention (Gnadt and Andersen, 1988), engage in monitoring feedback motor signals (corollary discharge) from motor areas, e.g. the frontal eye fields (Andersen *et al*., 1987; Duhamel *et al*., 1992*a*, *b*; Paus *et al*., 1995), engage in monitoring an eye position signal relative to the orbits (Andersen and Mountcastle, 1983; Andersen *et al*., 1985*b*) or represent automatic eye movement-related shifts of attention.

To locate visual objects accurately in extrapersonal space we are faced with the dilemma of distinguishing between a change in the location of a retinal image caused by a change in the direction of gaze and the same change caused by an actual displacement of the object in the visual field. The solution could arise from neurons of the visual system that

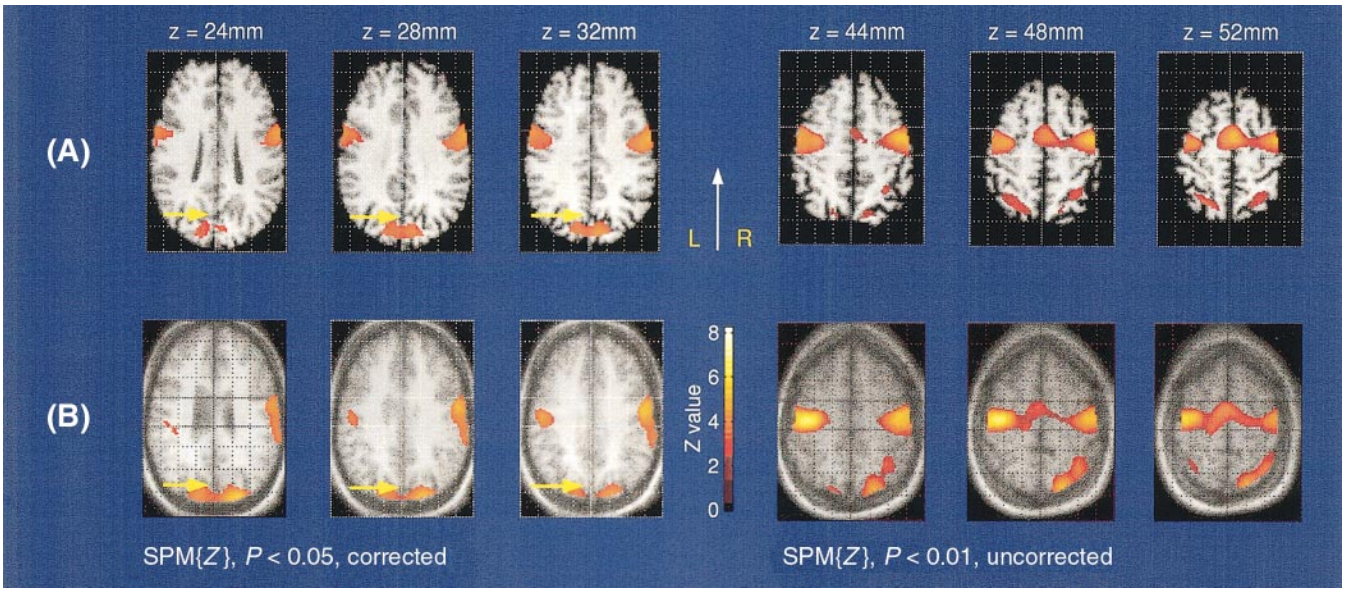

Fig. 4 The top row shows the group analysis (SPM{*Z*}) of all saccade scans compared with rest in the hypothesis-generating group (group A). The spatial extent of significantly activated areas is for anatomical reference superimposed on a single MRI template in coregistration with the stereotaxic atlas of Talairach and Tournoux (1988). In the bottom row the corresponding activation patterns for the hypothesis-testing group (group B) are shown for comparison superimposed on the group average of their stereotaxically normalized MRI scans. The images to the left show slices $z = 24$ mm to 32 mm above the AC–PC line at a significance threshold of $P < 0.05$, corrected. The replication of the activation of the cunei at the posterior bank of the parieto-occipital sulcus is seen. The yellow arrows point to the parieto-occipital sulcus. Slices $z = 44$ mm to 52 mm above the AC–PC line are displayed to the right at a significance threshold of $P < 0.01$, uncorrected ($Z > 2.33$). Of particular interest is the activation of the posterior parietal cortex close to and in the intraparietal sulci.

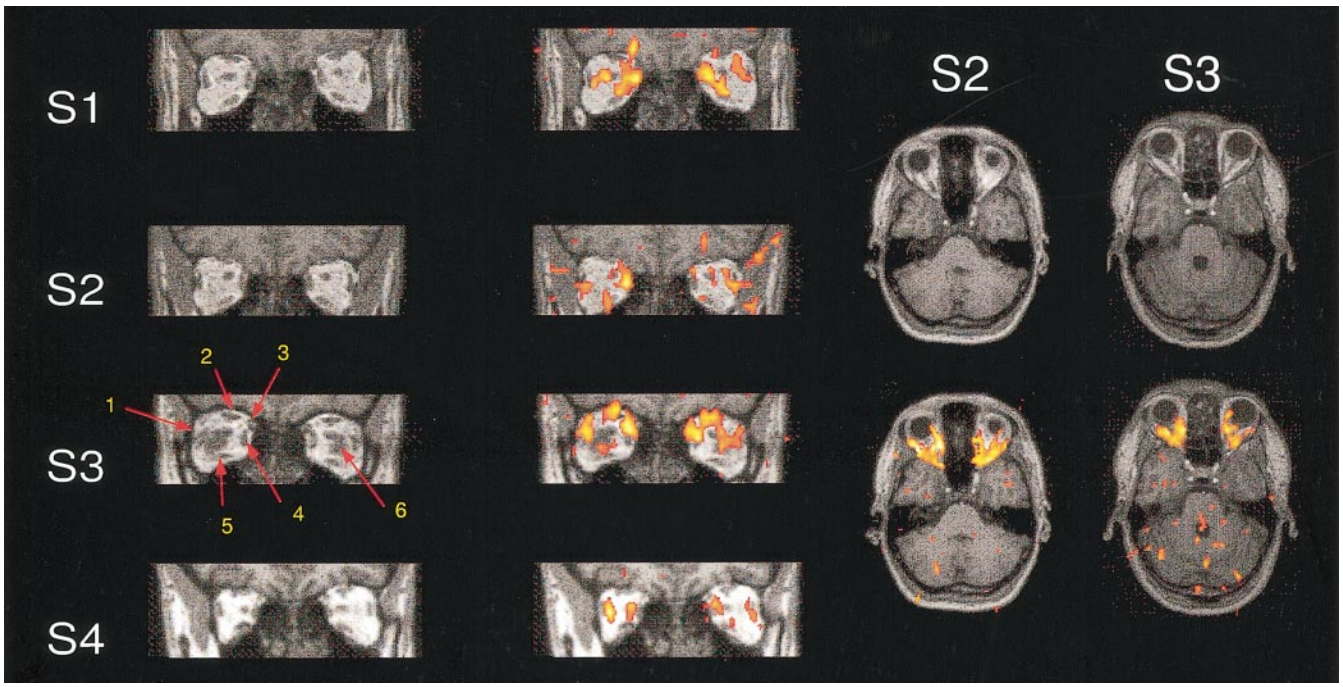

Fig. 5 Coronal anatomical MRI references through the orbital cavities of the four individual subjects in group B (S1–S4) (far left) and corresponding projections of the individual *Z* score maps calculated with only the PET scanner reconstruction filters (middle left). Transaxial slices of two selected subjects (S2–S3) in a similar display are shown on the right. The activated areas are scaled from *Z* values of 1.64–5.0. The activated areas were primarily located close to the apex of the pyramidal shaped orbital cavity, and had the largest *Z* scores in each individual comparison calculated in this fashion. The eye muscles (1–5) and ocular bulb/optic nerve (6) can easily be discerned, embedded in the high-intensity white orbital fat. 1 = lateral rectus muscle; 2 = levator palpebrae superioris muscle and superior rectus muscle; 3 = superior oblique muscle; 4 = medial rectus muscle; 5 = inferior rectus muscle and inferior oblique muscle.

integrate retinotopically organized visual information from their receptive fields and information about gaze direction (Galletti *et al*., 1993). Neurons sensitive to the position of the eyes in the orbits have been found in the nucleus prepositus hypoglossi in the brainstem (Lopez-Barneo *et al*., 1982), superior colliculus (Peck *et al*., 1980) and central thalamus (Schlag *et al*., 1980) of the cat, as well as in the cerebellar vermis (McElligott and Keller, 1984), extrastriate area V3A (Galletti and Battaglini, 1989), parieto-occipital area PO (V6) (Galletti *et al*., 1991, 1995), inferior parietal lobe (Sakata *et al*., 1980; Andersen and Mountcastle, 1983) and the supplementary eye field (Schall *et al*., 1993) of the monkey.

Based on cytoplasmic and myelin architecture in post-mortem human brains, the heavily myelinated dorsal area V3 (V3d) has been tentatively located 'lateral and superior to area V2 in the upper part of the occipital cortex' (the cuneus) (Clarke and Miklossy, 1990). This anatomical location has been confirmed by PET (Shipp *et al*., 1995) and functional MRI (Sereno *et al*., 1995; DeYoe *et al*., 1996). The functional MRI studies were performed using phase-encoded retinal stimulation, which locates area V3A rostral to area V3 behind the parieto-occipital sulcus. In the macaque monkey the extrastriate visual area PO (V6) has been located in the parieto-occipital sulcus close to area V3A (Colby *et al*., 1988). Both these areas include gaze-dependent neurons that even in darkness combine information about eye position with a restricted retinal receptive field (Galletti and Battaglini, 1989; Galletti *et al*., 1995, 1996). The high-frequency, large amplitude shifts performed by our subjects would involve a larger population of gaze-dependent neurons than that involved during rest, contributing to the observed signal increase. Thus, the activation of the cuneus could represent activation of either or both of these extrastriate visual areas.

In the macaque monkey, particularly the lateral part of the intraparietal sulcus has been associated with saccadic eye movements through strong connections to the SC and the frontal eye field (Andersen *et al*., 1985*a*; Huerta *et al*., 1987). The inferior parietal lobe does have the capacity to generate saccades by direct electrical stimulation, as demonstrated in 1875 by Ferrier and subsequently by others (Shibutani *et al*., 1984; Thier and Andersen, 1996), presumably accessing the brainstem saccade generator via either the frontal eye fields or the SC (Keating and Gooley, 1988). However, as very few saccade neurons have the correct temporal sequencing or response properties it is more likely that the saccade-related activity in the parietal lobe represents efferent motor command copies rather than motor commands and/or proprioceptive input from the extraocular muscles relaying information about the occurrence of an eye movement (Andersen *et al*., 1987). In a recent PET experiment, Paus *et al*. (1997) activated the left frontal eye field by focal TMS (transcranial magnetic stimulation). This activation showed significant covariation with the ipsilateral medial parieto-occipital cortex in the cuneus immediately posterior to the parieto-occipital sulcus [(x, y, z) = (–12, –80, 30)], i.e. at a location identical to ours. Since this procedure is independent of a given behavioural set the activations are likely to represent efferent copies powerful enough to elicit detectable changes with PET. The functional significance of the efferent feedback copies could be to anticipate the retinal consequences of eye movements and provide a continuous remapping of the representation of visual space (Duhamel *et al*., 1992*a*).

The eye movement artefact

The individual SPM analysis of the original PET images projected on to the corresponding structural MRI scans in group B confirmed that the activation observed close to the orbitofrontal cortices was an artefact. The artefact presumably arose from eye movement-induced blood flow increases in the six external eye muscles of the orbital cavities (Fig. 5) with spill-over into the adjacent cortical areas. This effect is enhanced by the filtering process involved in the SPM approach, which, due to the proximity to the orbitofrontal cortex, is inefficiently excluded by the 80% grey matter threshold. Artefacts arising from muscle blood flow increases are known sources of error in methods relying on the measurement of rCBF. Previously, increased tone in the muscles of mastication during anxiety attacks has erroneously been interpreted as activation of the parahippocampal gyri (Reiman *et al*., 1984) or the temporal poles (Reiman *et al*., 1989; Drevets *et al*., 1992).

The artefact has been deliberately included in the data presentation as it has not been described before, in order to increase awareness of its spatial extent and configuration should it be present in future studies. The absence of the artefact in previous PET studies is presumably due to the restricted axial fields of view of the scanners involved.

Conclusion

Our study demonstrates that the presentation of overt visual stimuli during eye movements is not a prerequisite for the activation of the extrastriate visual cortex, the cuneus and possibly the intraparietal sulcus. Note that no other visual areas were activated. It is thus supportive of the concept that these areas are involved in the reception and integration of motor efferent copies and/or eye position signals. These are important constituents of the location and remapping of visual stimuli in space. This would indicate that a segment of the activations of this area during visually guided saccadic eye movements found previously (Anderson *et al*., 1994; Sweeney *et al*., 1996; Law *et al*., 1997) can be attributed to corollary discharge and/or eye position signals associated with the performance of eye movements *per se* apart from the activation arising from the visuospatial task components.

Furthermore, our results indicate that specific attention should be paid to the possibility of misinterpreting extraocular muscle blood flow increases as activations of the orbitofrontal cortices.

Acknowledgements

The authors wish to thank Karin Stahr and the staff at the PET centre at Rigshospitalet, Copenhagen, for their participation. This work was supported by a grant from the Danish Medical Research Council and the Danish Foundation for the Advancement of Medical Science.

References

Andersen RA. Inferior parietal lobule function in spatial perception and visuomotor integration. In: Mountcastle VB, Plum F, editors. Handbook of physiology, Sect 1, Vol. 5, Pt 2. Bethesda (MD): American Physiological Society; 1987. p. 483–518.

Andersen RA, Mountcastle VB. The influence of the angle of gaze upon the excitability of the light-sensitive neurons of the posterior parietal cortex. J Neurosci 1983; 3: 532–48.

Andersen RA, Asanuma C, Cowan WM. Callosal and prefrontal associational projecting cell populations in area 7A of the macaque monkey: a study using retrogradely transported fluorescent dyes. J Comp Neurol 1985a; 232: 443–55.

Andersen RA, Essick GK, Siegel RM. Encoding of spatial location by posterior parietal neurons. Science 1985b; 230: 456–8.

Andersen RA, Essick GK, Siegel RM. Neurons of area 7 activated by both visual stimuli and oculomotor behavior. Exp Brain Res 1987; 67: 316–22.

Anderson TJ, Jenkins IH, Brooks DJ, Hawken MB, Frackowiak RS, Kennard C. Cortical control of saccades and fixation in man. A PET study. Brain 1994; 117: 1073–84.

Ardekani BA, Braun M, Hutton BF, Kanno I, Iida H. A fully automatic multimodality image registration algorithm. J Comput Assist Tomogr 1995; 19: 615–23.

Barash S. Area LIP and the population vector: single and double targets. In: Thier P, Karnath HO, editors. Parietal lobe contributions to orientation in 3D space. Berlin: Springer; 1997. p. 109–35.

Clarke S, Miklossy J. Occipital cortex in man: organization of callosal connections, related myelo- and cytoarchitecture, and putative boundaries of functional visual areas. J Comp Neurol 1990; 298: 188–214.

Colby CL, Gattass R, Olson CR, Gross CG. Topographical organization of cortical afferents to extrastriate visual area PO in the macaque: a dual tracer study. J Comp Neurol 1988; 269: 392–413.

Darby DG, Nobre AC, Thangaraj V, Edelman R, Mesulam MM, Warach S. Cortical activation in the human brain during lateral saccades using EPISTAR functional magnetic resonance imaging. Neuroimage 1996; 3: 53–62.

DeGrado TR, Turkington TG, Williams JJ, Stearns CW, Hoffman JM, Coleman RE. Performance characteristics of a whole-body PET scanner. J Nucl Med 1994; 35: 1398–406.

DeYoe EA, Carman GJ, Bandettini P, Glickman S, Wieser J, Cox R, et al. Mapping striate and extrastriate visual areas in human cerebral cortex. Proc Natl Acad Sci USA 1996; 93: 2382–6.

Drevets WC, Videen TQ, MacLeod AK, Haller JW, Raichle ME. PET images of blood flow changes during anxiety: correction [letter]. Science 1992; 256: 1696.

Duhamel JR, Colby CL, Goldberg ME. The updating of the representation of visual space in parietal cortex by intended eye movements. Science 1992a; 255: 90–2.

Duhamel JR, Goldberg ME, Fitzgibbon EJ, Sirigu A, Grafman J. Saccadic dysmetria in a patient with a right frontoparietal lesion. The importance of corollary discharge for accurate spatial behaviour. Brain 1992b; 115: 1387–402.

Ferrier D. Experiments on the brain of monkeys. Proc R Soc 1875; 23: 409–30.

Fox PT, Mintun MA. Noninvasive functional brain mapping by change-distribution analysis of averaged PET images of $H_2{}^{15}O$ tissue activity. J Nucl Med 1989; 30: 141–9.

Fox PT, Fox JM, Raichle ME, Burde RM. The role of cerebral cortex in the generation of voluntary saccades: a positron emission tomographic study. J Neurophysiol 1985; 54: 348–69.

Frackowiak RS, Friston KJ. Functional neuroanatomy of the human brain: positron emission tomography—a new neuroanatomical technique. [Review]. J Anat 1994; 184: 211–25.

Friston KJ. Statistical parametric mapping. In: Thatcher RW, Hallett M, Zeffiro T, Roy John E, Huerta M, editors. Functional neuroimaging: technical foundations. San Diego: Academic Press; 1994. p. 79–93.

Friston KJ, Frith CD, Liddle PF, Frackowiak RS. Comparing functional (PET) images: the assessment of significant change. J Cereb Blood Flow Metab 1991; 11: 690–9.

Friston KJ, Ashburner J, Frith CD, Poline JB, Heather JD, Frackowiak RSJ. Spatial registration and normalization of images. Hum Brain Mapp 1995a; 3: 165–89.

Friston KJ, Holmes AP, Worsley KJ, Poline JB, Frith CD, Frackowiak RSJ. Statistical parametric maps in functional imaging: a general linear approach. Hum Brain Mapp 1995b; 2: 189–210.

Galletti C, Battaglini PP. Gaze-dependent visual neurons in area V3A of monkey prestriate cortex. J Neurosci 1989; 9: 1112–25.

Galletti C, Battaglini PP, Fattori P. Functional properties of neurons in the anterior bank of the parieto-occipital sulcus of the macaque monkey. Eur J Neurosci 1991; 3: 452–61.

Galletti C, Battaglini PP, Fattori P. Cortical mechanisms of visual space representation. Biomed Res Japan 1993; 4.

Galletti C, Battaglini PP, Fattori P. Eye position influence on the parieto-occipital area PO (V6) of the macaque monkey. Eur J Neurosci 1995; 7: 2486–501.

Galletti C, Fattori P, Battaglini PP, Shipp S, Zeki S. Functional demarcation of a border between areas V6 and V6A in the superior parietal gyrus of the macaque monkey. Eur J Neurosci 1996; 8: 30–52.

Gnadt JW, Andersen RA. Memory related motor planning activity in posterior parietal cortex of macaque. Exp Brain Res 1988; 70: 216–20.

Haxby JV, Grady CL, Horwitz B, Ungerleider LG, Mishkin M, Carson RE, et al. Dissociation of object and spatial visual processing

pathways in human extrastriate cortex. Proc Natl Acad Sci USA 1991; 88: 1621–5.

Huerta MF, Krubitzer LA, Kaas JH. Frontal eye field as defined by intracortical microstimulation in squirrel monkeys, owl monkeys, and macaque monkeys. II. Cortical connections. J Comp Neurol 1987; 265: 332–61.

Iida H, Kanno I, Miura S. Rapid measurement of cerebral blood flow with positron emission tomography. Ciba Found Symp 1991; 163: 23–37.

Kanno I, Iida H, Miura S, Murakami M. Optimal scan time of oxygen-15-labeled water injection method for measurement of cerebral blood flow [see comments]. J Nucl Med 1991; 32: 1931–4. Comment in: J Nucl Med 1991; 32: 1934–6.

Keating EG, Gooley SG. Disconnection of parietal and occipital access to the saccadic oculomotor system. Exp Brain Res 1988; 70: 385–98.

Law I, Svarer C, Holm S, Paulson OB. The activation pattern in normal humans during suppression, imagination and performance of saccadic eye movements. Acta Physiol Scand 1997; 161: 419–34.

Lopez-Barneo J, Darlot C, Berthoz A, Baker R. Neuronal activity in prepositus nucleus correlated with eye movement in the alert cat. J Neurophysiol 1982; 47: 329–52.

McElligott JG, Keller EL. Cerebellar vermis involvement in monkey saccadic eye movements: microstimulation. Exp Neurol 1984; 86: 543–58.

Melamed E, Larsen B. Cortical activation pattern during saccadic eye movements in humans: localization by focal cerebral blood flow increases. Ann Neurol 1979; 5: 79–88.

Mishkin M, Ungerleider LG, Macko KA. Object vision and spatial vision: two cortical pathways. Trends Neurosci 1983; 6: 414–7.

Mountcastle VB, Lynch JC, Georgopoulos A, Sakata H, Acuna C. Posterior parietal association cortex of the monkey: command functions for operations within extrapersonal space. J Neurophysiol 1975; 38: 871–908.

Nakashima Y, Momose T, Sano I, Katayama S, Nakajima T, Niwa S, et al. Cortical control of saccade in normal and schizophrenic subjects: a PET study using a task-evoked rCBF paradigm. Schizophr Res 1994; 12: 259–64.

O'Driscoll GA, Alpert NM, Matthysse SW, Levy DL, Rauch SL, Holzman PS. Functional neuroanatomy of antisaccade eye movements investigated with positron emission tomography. Proc Natl Acad Sci USA 1995; 92: 925–9.

O'Sullivan EP, Jenkins IH, Henderson L, Kennard C, Brooks DJ. The functional anatomy of remembered saccades: a PET study. Neuroreport 1995; 6: 2141–4.

Oldfield RC. The assessment and analysis of handedness: the Edinburgh inventory. Neuropsychologia 1971; 9: 97–113.

Paus T, Petrides M, Evans AC, Meyer E. Role of the human anterior cingulate cortex in the control of oculomotor, manual, and speech responses: a positron emission tomography study. J Neurophysiol 1993; 70: 453–69.

Paus T, Marrett S, Worsley KJ, Evans AC. Extraretinal modulation of cerebral blood flow in the human visual cortex: implications for saccadic suppression. J Neurophysiol 1995; 74: 2179–83.

Paus T, Jech R, Thompson CJ, Comeau R, Peters T, Evans AC. Transcranial magnetic stimulation during positron emission tomography: a new method for studying connectivity of the human cerebral cortex. J Neurosci 1997; 17: 3178–84.

Peck CK, Schlag-Rey M, Schlag J. Visuo-oculomotor properties of cells in the superior colliculus of the alert cat. J Comp Neurol 1980; 194: 97–116.

Petit L, Orssaud C, Tzourio N, Salamon G, Mazoyer B, Berthoz A. PET study of voluntary saccadic eye movements in humans: basal ganglia–thalamocortical system and cingulate cortex involvement. J Neurophysiol 1993; 69: 1009–17.

Petit L, Orssaud C, Tzourio N, Crivello F, Berthoz A, Mazoyer B. Functional anatomy of a prelearned sequence of horizontal saccades in humans. J Neurosci 1996; 16: 3714–26.

Reiman EM, Raichle ME, Butler FK, Herscovitch P, Robins E. A focal brain abnormality in panic disorder, a severe form of anxiety. Nature 1984; 310: 683–5.

Reiman EM, Fusselman MJ, Fox PT, Raichle ME. Neuroanatomical correlates of anticipatory anxiety [published erratum appears in Science 1992; 256: 1696]. Science 1989; 243: 1071–4.

Sakata H, Shibutani H, Kawano K. Spatial properties of visual fixation neurons in posterior parietal association cortex of the monkey. J Neurophysiol 1980; 43: 1654–72.

Schall JD. Neural basis of saccadic eye movements in primates. In: Leventhal AG, editor. The neural basis of visual function. London: Macmillan Press; 1991a. p. 388–442.

Schall JD. Neuronal activity related to visually guided saccades in the frontal eye fields of rhesus monkeys: comparison with supplementary eye fields. J Neurophysiol 1991b; 66: 559–79.

Schall JD. Neuronal activity related to visually guided saccadic eye movements in the supplementary motor area of rhesus monkeys. J Neurophysiol 1991c; 66: 530–58.

Schall JD, Morel A, Kaas JH. Topography of supplementary eye field afferents to frontal eye field in macaque: implications for mapping between saccade coordinate systems. Vis Neurosci 1993; 10: 385–93.

Schlag J, Schlag-Rey M, Peck CK, Joseph JP. Visual responses of thalamic neurons depending on the direction of gaze and the position of targets in space. Exp Brain Res 1980; 40: l70–84.

Sereno MI, Dale AM, Reppas JB, Kwong KK, Belliveau JW, Brady TJ, et al. Borders of multiple visual areas in humans revealed by functional magnetic resonance imaging [see comments]. Science 1995; 268: 889–93. Comment in: Science 1995; 268: 803–4.

Shibutani H, Sakata H, Hyvarinen J. Saccade and blinking evoked by microstimulation of the posterior parietal association cortex of the monkey. Exp Brain Res 1984; 55: 1–8.

Shipp S, Watson JDG, Frackowiak RSJ, Zeki S. Retinotopic maps in human prestriate visual cortex: the demarcation of areas V2 and V3. Neuroimage 1995; 2: 125–32.

Silbersweig DA, Stern E, Frith CD, Cahill C, Schnorr L, Grootoonk S, et al. Detection of thirty-second cognitive activations in single

subjects with positron emission tomography: a new low-dose H2(15)O regional cerebral blood flow three-dimensional imaging technique. J Cereb Blood Flow Metab 1993; 13: 617–29.

Sweeney JA, Mintun MA, Kwee S, Wiseman MB, Brown DL, Rosenberg DR, et al. Positron emission tomography study of voluntary saccadic eye movements and spatial working memory. J Neurophysiol 1996; 75: 454–68.

Talairach J, Tournoux P. Co-planar stereotaxic atlas of the human brain. Stuttgart: Thieme; 1988.

Thier P, Andersen RA. Electrical microstimulation suggests two different forms of representation of head-centered space in the intraparietal sulcus of rhesus monkeys. Proc Natl Acad Sci USA 1996; 93: 4962–7.

Woods RP, Cherry SR, Mazziotta JC. Rapid automated algorithm for aligning and reslicing PET images. J Comput Assist Tomogr 1992; 16: 620–33.

Received March 16, 1998. Accepted June 4, 1998